Proceedings Paper:
Chudpooti, N, Sangpet, P, Duangrit, N et al. (3 more authors) (2021) An Integrated 3D-Printed Lens with Ultra-Wideband Flower-Shaped Stub Antenna for Ethanol-Water Mixture Characterization. In: 2021 Research, Invention, and Innovation Congress: Innovation Electricals and Electronics (RI2C). 2021 Research, Invention, and Innovation Congress: Innovation Electricals and Electronics (RI2C), 01-03 Sep 2021, Bangkok, Thailand. IEEE , pp. 80-83. ISBN 978-1-6654-0300-9

https://doi.org/10.1109/ri2c51727.2021.9559770

An Integrated 3D-Printed Lens with Ultra-Wideband Flower-Shaped Stub Antenna for Ethanol-Water Mixture Characterization

Nonchanutt Chudpooti
Department of Industrial Physics and Medical Instrumentation, Facutly of Appied Science, King Mongkut's University of Technology North Bangkok
Bangkok, Thailand
nonchanutt.c@sci.kmutnb.ac.th

Patchadaporn Sangpet
Deparment of Electrical and Computer Engineering, Faculty of Engineering King Mongkut's University of Technology North Bangkok
Bangkok, Thailand
s.patchadaporn@gmail.com

Nattapong Duangrit
Faculty of Engineering Rajamangala University of Technology Lanna
Chiangmai, Thailand
nattapong.du@rmutl.ac.th

Prayoot Akkaraekthalin
Deparment of Electrical and Computer Engineering, Faculty of Engineering King Mongkut's University of Technology North Bangkok
Bangkok, Thailand
prayoot.a@eng.kmutnb.ac.th

Ian D. Robertson
School of Electronic and Electrical Engineering University of Leeds
Leeds, U.K.
i.d.robertson@leeds.ac.uk

Nutapong Somjit
School of Electronic and Electrical Engineering University of Leeds
Leeds, U.K.
n.somjit@leeds.ac.uk

***Abstract*— This paper presents a 3D-printed hemispherical lens integrated with flower-shaped stub antenna for liquid-mixture characterization. The proposed lens antenna is designed, fabricated, and integrated with the ultra-wideband planar antenna. A high impact polystyrene (HIPs) is selected to design the 3D-printed lens antenna by using the fused deposition modelling (FDM) technique, due to low loss 3D-printed material. The optimum the dimensions of the lens antenna are obtained by using the 3D EM Simulation CST Studio, which is used to investigate the performance of the antenna, e.g., gain, radiation pattern and reflection coefficient. To discriminate the liquid content in ethanol-water mixture, the level of the transmission coefficient (S_{21}) is detected. The proposed sensor system offers various preferable features, e.g., non-destructive method and non-contact measurement. Five samples, e.g., 60%, 65%, 70%, 75%, and 80% ethanol in the ethanol-water mixtures, are measured and performed to generate the extraction model. The proposed sensor also offers other advantages, e.g., real-time monitoring and no life-cycle limitation.**

Keywords*— *liquid-mixture characterization, 3D-printed lens antenna, non-destructive measurement, real-time monitoring

I. Introduction

The microwave and millimeter-wave sensors have become attractive techniques in liquid-mixture concentration characterization, which are applied to many systems such as industrial, biomedical, and biological applications [1]-[9]. The microwave measurement techniques provide many advantages, i.e., real-time monitoring, high sensitivity, non-destructive method, not require any chemical processes, etc. Two microwave characterization techniques, e.g., transmission-line and resonance techniques, are mostly used to apply in microwave sensor systems. The transmission-line technique is mostly used for broadband material characterization [1]. On the other hand, the resonance technique offers high precision and accuracy. This technique is often used in discrete frequency or narrow band [2]. For instance, a tailor-made *H*-plane split rectangular waveguide, operating at 90 GHz, is designed for discriminating the level of the ethanol concentration in the DI-water liquid-mixture content [1]. In [1], the sensors provide high sensitivity by discriminating ethanol content of approximately 2% in the liquid mixture. Additionally, in [3], the modified *H*-plane split waveguide is designed for detecting the thickness of the photoresist film by using the resonance technique. The extracted results can discriminate the level of SU-8 layer in micrometer scale.

The additive manufacturing process provides enhanced flexibility in choosing the dielectric material to be used as the hollow substrate. It has advantages of stability, ease of design, low-cost, lightweight, and the possibility for mechanical flexibility. It offers a new degree of design freedom for applications benefitting from the use of conformal and flexible structures [10]-[13]. The 3D printing technology, also known as additive manufacturing, is defined as the development of an arbitrary 3D shape, by building layer upon layer. Based on 3D printing technology, there are many techniques, e.g., fused deposition modeling (FDM), polymer jetting (PolyJet) and digital light processing (DLP). However, due to a performance in fabricating high-accuracy 3D structures and various choices of printing materials, the DLP technique is often preferred to FDM and PolyJet fabrication.

This paper presents 3D-printed lens antennas using the FDM technique to improve the antenna characteristic of a flower-shaped stub antenna. The 3D-printed hemispherical lens antennas are designed for integrating with a flower-shaped stub antenna without any adhesive layer. To characterize the percentage of the liquid content in the liquid mixture, the transmission line technique is used due to broadband measurement and is suitable for lossy materials. The proposed antennas are placed between the liquid under test (LUT). The space between the sample and antennas is optimized by using 3D EM Simulation CST Studio. Five samples, e.g., 60%, 65%, 70%, 75%, and 80% ethanol in the ethanol/water mixtures, are measured. The proposed system offers various preferable features, e.g., non-destructive method and non-contact measurement.

II. Antenna Design and Fabrication

A. Ultra-Wideband Flower-Shaped Stub Antenna

The flower-shaped stub antenna has been published in [14]. This antenna was designed for supporting ultra-

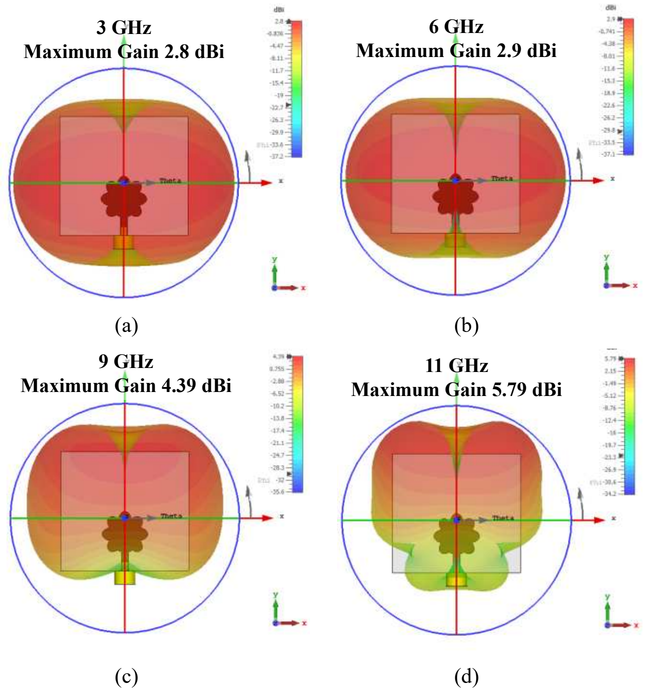

Fig. 1. The simulated 3D radiation pattern of the original ultra-wideband flower-shaped stub antenna at (a) 3 GHz, (b) 6 GHz, (c) 9 GHz and (d) 11 GHz.

wideband (UWB) applications. The operating frequency starts from 3 GHz to 12.5 GHz with a compact size of 16 mm × 24 mm. This antenna is fabricated by using an FR-4 substrate with a thickness, S_t, of 0.8 mm. The design and geometry of this antenna are used in [14]. Figure 1 shows the simulated 3D radiation pattern of four frequencies, e.g., 3 GHz, 6 GHz, 9 GHz, and 11 GHz, which has the maximum realized gain of 2.8 dBi, 2.9 dBi, 4.39 dBi, and 5.79 dBi, respectively. Based on simulated results, at the higher frequency, the maximum gain does not confine at the center antenna (zero-degree). To improve the antenna characteristic and control the antenna beam, the 3D-printed hemispherical lens antennas are designed in *part B*.

B. 3D-Printed Hemisphical Lens Antennas

The 3D-printed hemispherical lens antenna is designed based on the FDM printing method. The high impact polystyrenes (HIPS) material is used to design the lens antenna due to its low cost, low profile, and materials available in the laboratory. In [10], a relative permittivity, ε_r, and loss factor, *tan δ*, of the HIPS material, has been reported, which are 2.45 and $5.75{\times}10^{-4}$, respectively. Figure 2 shows the geometry of the ultra-wideband flower-shaped stub antenna with 3D-printed hemispherical lens antennas. The ratio of the lens radius, R_{lens}, and extension length, L_{lens}, which were reported in [10], is fixed at 1 to get maximum gain. The optimum dimensions of the lens antenna are obtained by using the 3D EM Simulation CST Studio, which is used to investigate the performance of the antenna, e.g., gain, radiation pattern, and reflection coefficient. The lens radius, R_{lens}, and extension length, L_{lens}, have the same value of 12 mm. The width, W_h, and length, L_h, of the 3D-printed case, are 30 mm and 27 mm, respectively. The thickness of the 3D-printed case is 5.835 mm. The gap, g, is controlled to reduce the reflection coefficient, S_{11}. The gap, g, is set to 3 mm.

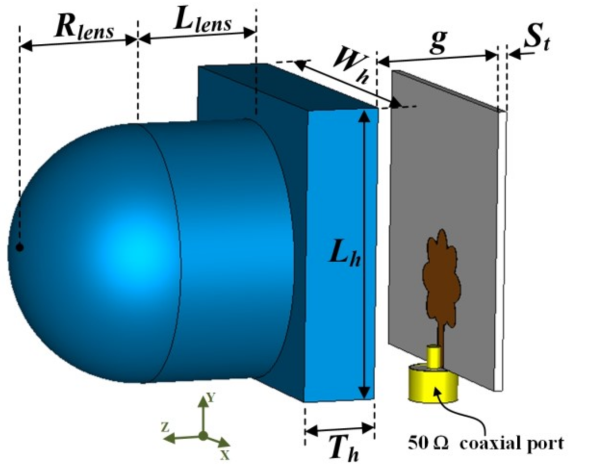

Fig. 2. The geometry of the ultra-wideband flower-shaped stub antenna integrated with 3D-printed lens antennas.

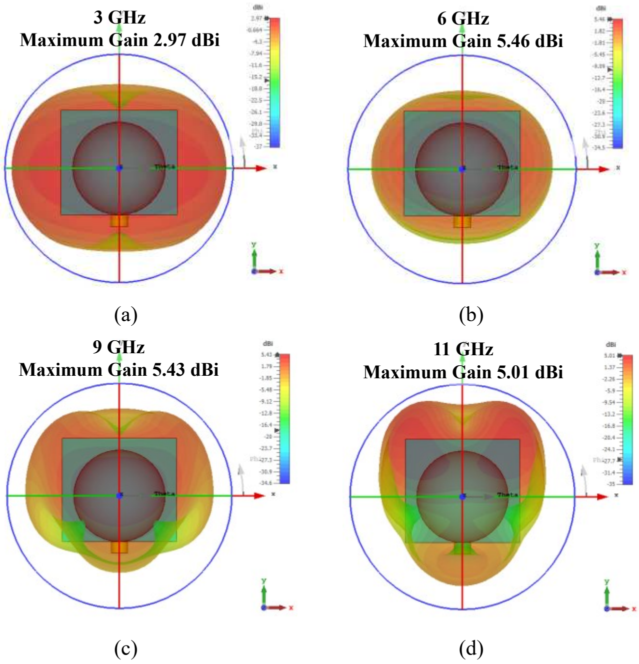

Fig. 3. The simulated 3D radiation pattern of the Integrated 3D-Printed Lens with ultra-wideband flower-shaped stub antenna at (a) 3 GHz, (b) 6 GHz, (c) 9 GHz and (d) 11 GHz.

Figure 3 shows the simulated realized gain antenna after assembly of the 3D-printed lens antennas with UWB flower-shaped stub antenna. Four frequencies are selected to show the shape and direction of the pattern. The maximum realized gain at 3 GHz, 6 GHz, 9 GHz, and 11 GHz, are 2.97 dBi, 5.46 dBi, 5.43 dBi, and 5.01 dBi, respectively. The antenna gain at zero degrees is improved after integrating a 3D-printed lens antenna.

C. 3D-printed Lens Fabricaiton and Assembly

The proposed lens antenna is fabricated by using the FDM manufacturing technique. The Zortrax M200, which is an available 3D-printing machine in the laboratory, is selected to run the 3D-printed hemispherical lens antenna. The HIPS is mostly used for printing a model that requires a smooth surface. The Z-SUIT Zortrax is a commercial program to use for the setup of the 3D printing parameter. In this printing setup, a layer thickness is set to 90 μm. The diameter of the nozzle is 0.4 mm, and 100% infill density. Figures 4 show the before and after assembly of the UWB flower-shaped stub antenna and 3D-printed lens antennas.

III. Measurement results

A. Antenan Performance

A vector network analyzer, which is a Rohde & Schwarz ZVB-20 model, is used with Through-Open-Short-Match (TOSM) calibration to calculate the reflection coefficient, S_{11}, and radiation pattern of the fabricated 3D-printed lens antennas. Figure 5 shows the simulated and measured results of the reflection coefficient, S_{11}, over the band of 2 GHz to 12 GHz. The measured result shows that the reflection coefficient, S_{11}, has a value lower than 10 dB from 3.1 GHz to 10.5 GHz. To measure the radiation pattern of the fabricated lens antenna, a standard horn antenna with an average gain of 15 dBi was used as the reference antenna. The DAMs Heavy-Duty Antenna Model-5100, which is a turntable for rotating the antenna under test (AUT), was connected with the Rohde & Schwarz ZVB-20. The Diamond Studio Suite software is used to manage and accumulate the transmission coefficient, S_{21}, between the reference antenna and the AUT. Figure 6 shows the comparison of the measured results at the zero-degree in case of with and without integrated 3D-printed hemispherical lens antenna. From the measurement result, the antenna gains of the 3D-printed lens antenna have an average gain of 5.6 dBi, while the original flower-shaped stub antenna has an average gain of 0.67 dBi.

B. Measurement Setup and Results

The *S*-parameter measurements were performed by using a ROHDE & SCHWARZ ZVB-20 Vector Network Analyzer (VNA). Two-port calibration technique was performed using the Thru-Open-Short-Match method (TOSM), in order to eliminate the systematic errors contributed by the VNA and connecting cables. The frequency range of the VNA was set from 9 GHz to 11 GHz. The number of sampling frequency points was 2,001 points. The intermediate frequency (IF) filter bandwidth was set to 1 kHz. Figure 7 shows the measurement setup of the liquid mixture characterization. Two fabricated 3D-printed hemispherical lens antennas are placed between LUT, which is filled in the glass bottle. The distance between the glass bottle and 3D-printed lens antennas, *L*, is fixed to 10 mm. The temperature of the liquid solution sample was well maintained at a room temperature of 25 degrees Celsius. At least five repeated individual measurements were conducted to ensure the measurement and sensor repeatability.

Figure 8 shows the measured results of the transmission coefficient, S_{21}, of six conditions, e.g., empty solution, ethanol 60%, ethanol 65%, ethanol 70%, ethanol 75%, and ethanol 80%. From measurement results, focusing at 9.90 GHz, the transmission coefficient, S_{21}, of the empty solution is -5.71 dB. When filling the liquid solutions, the level of the transmission coefficient, S_{21}, will drop, which depends on the percentage of the ethanol in the ethanol/water liquid mixture. The levels of the transmission coefficient, S_{21}, when filling the liquid solution of 60% ethanol, 65 % ethanol, 70 % ethanol, 75 % ethanol, and 80 % ethanol, are -20.46 dB, -18.95 dB, -18.02 dB, -17.12 dB, and -15.76 dB, respectively. Based on measurement results, the trend of the proposed system can conclude that when increasing the percentage of ethanol, the level of the transmission coefficient, S_{21}, will shift down.

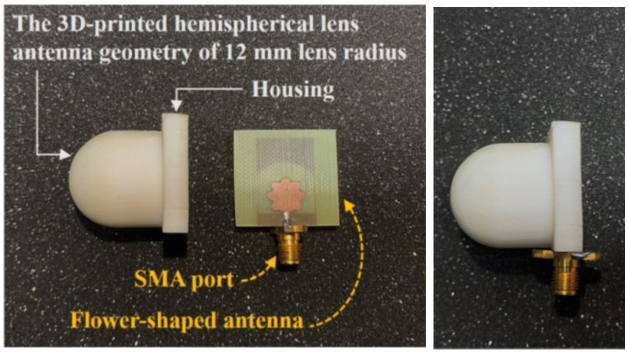

Fig. 4. The fabricated ultra-wideband flower-shaped stub antenna and 3D-printd lens antenna (a) before assembly and (b) after assembly.

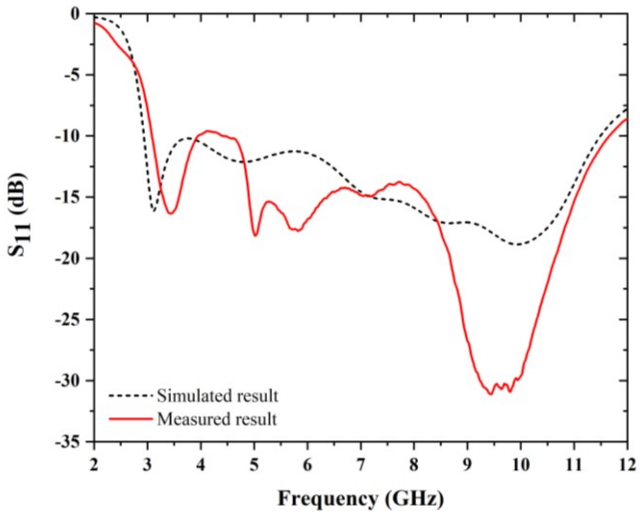

Fig. 5. The simulated and measured results of the reflection coefficient, S_{11}, when embedding the 3D-printed hemispherical lens antenna.

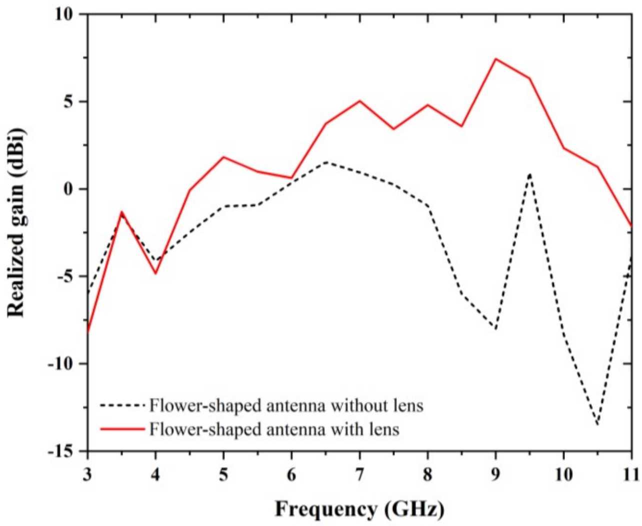

Fig. 6. The measured gain at 0 degree of the ultra-wideband flower-shaped stub antenna with and without 3D-printed hemispherical lens antenna.

IV. Conclusion

This paper reports 3D-printed hemispherical lens antennas integrated with UWB flower-shaped stub antenna for improve the antenna characteristics, e.g., reflection coefficient, S11, and antenna gain. The 3D-printed hemispherical lens antennas

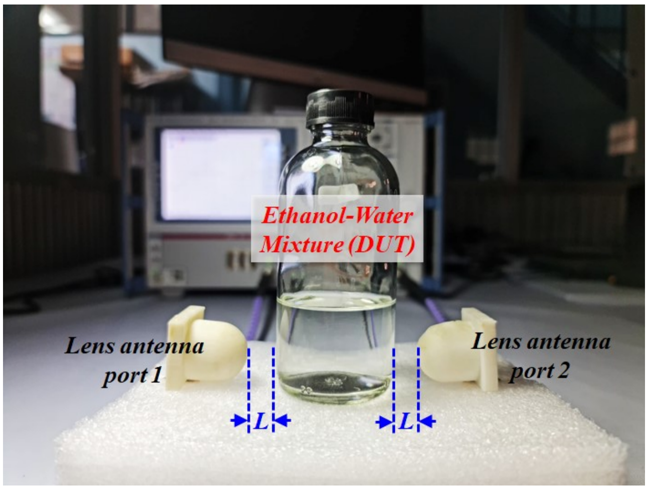

Fig. 7. The 3D-printed lens antennas are setup by placing between the DUT. The distance between lens antenna and DUT is set to 10 mm.

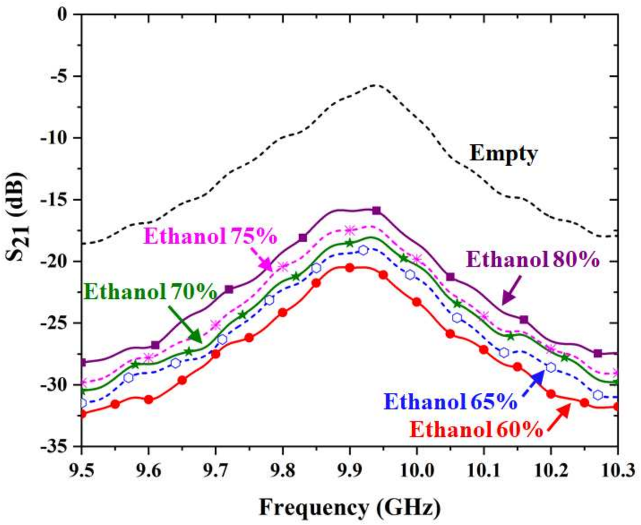

Fig. 8. The measured results of the transmission coefficient, S_{21}, of Six conditions.

are designed for integrating with a flower-shaped stub antenna without any adhesive layer. The average antenna gain at the zero-degree is increased from 0.67 dBi to 5.6 dBi after integrated 3D-printed lens antenna. The proposed antennas are placed between the liquid under test (LUT). Five solutions, e.g., 60%, 65%, 70%, 75%, and 80% ethanol in the ethanol/water mixtures, are measured. The proposed system provides various preferable features, e.g., non-destructive method and shot assay measurement time.

ACKNOWLEDGMENT

This work was supported funded by Thailand Science Research and Innovation Fund, and King Mongkut's University of Technology North Bangkok with contract no. KMUTNB-FF-65-42.

REFERENCES

[1] N. Chudpooti, E. Silavwe, P. Akkaraekthalin, I. D. Robertson and N. Somjit, “Nano-Fluidic Millimeter-Wave Lab-on-a-Waveguide Sensor for Liquid-Mixture Characterization,” *IEEE Sensors Journal*, vol. 18, no. 1, pp. 157-164, Jan., 2018.

[2] N. Chudpooti *et al.*, “In-Situ Self-Aligned NaCl-Solution Fluidic-Integrated Microwave Sensors for Industrial and Biomedical Applications,” *IEEE Access*, vol. 8, pp. 188897-188907, 2020.

[3] N. Chudpooti, V. Doychinov, P. Akkaraekthalin, I. D. Robertson and N. Somjit, “Non-Invasive Millimeter-Wave Profiler for Surface Height Measurement of Photoresist Films,” *IEEE Sensors Journal*, vol. 18, no. 8, pp. 3174-3182, April, 2018.

[4] N. Chudpooti, N. Duangrit and P. Akkaraekthalin, “A Miniaturized Planar Sensor Using Minkowski Fractal Technique for Material Characterization,” *2019 16th International Conference on Electrical Engineering/Electronics, Computer, Telecommunications and Information Technology (ECTI-CON)*, 2019, pp. 756-759.

[5] S. Seewattananpon, N. Promasa, N. Chudpooti and P. Akkaraekthalin, “Paddy Moisture Measurement System in Hopper Silo by using Near-field Transmission Technique,” *2018 International Symposium on Antennas and Propagation (ISAP)*, 2018, pp. 1-2.

[6] T. Pechrkool, N. Chudpooti, N. Duangrit, S. Chaimool and P. Akkaraekthalin, “Zeroth-Order Resonator Based on Mushroom-like Structure for Liquid Mixture Concentration Sensing of Sodium Chloride Solution,” *2019 IEEE Conference on Antenna Measurements & Applications (CAMA)*, 2019.

[7] P. Akkaraekthalin *et al.*, “Electromagnetic-based Innovative Sensors for Industrial and Agricultural Applications,” *2020 IEEE International RF and Microwave Conference (RFM)*, 2020, pp. 1-4.

[8] N. Chudpooti, N. Duangrit, P. Akkaraekthalin, I. D. Robertson and N. Somjit, “Electronics-Based Free-Space Terahertz Measurement Using Hemispherical Lens Antennas,” *IEEE Access*, vol. 7, pp. 95536-95546, 2019.

[9] W. Krudpun, N. Chudpooti, P. Lorwongtragool, S. Seewattanapon and P. Akkaraekthalin, “PSE-Coated Interdigital Resonator for Selective Detection of Ammonia Gas Sensor,” *IEEE Sensors Journal*, vol. 19, no. 23, pp. 11228-11235, Dec., 2019.

[10] N. Chudpooti, N. Duangrit, P. Akkaraekthalin, I. D. Robertson and N. Somjit, “220-320 GHz Hemispherical Lens Antennas Using Digital Light Processed Photopolymers,” *IEEE Access*, vol. 7, pp. 12283-12290, 2019.

[11] N. Chudpooti, S. Praesomboon, N. Duangrit, N. Somjit and P. Akkaraekthalin, “An X-band Portable 3D-printed Lens Antenna with Integrated Waveguide Feed for Microwave Imaging,” *2019 PhotonIcs & Electromagnetics Research Symposium - Spring (PIERS-Spring)*, 2019, pp. 487-492.

[12] G. Savvides *et al.*, “3D Rapid-Prototyped 21-31-GHz Hollow SIWs for Low-Cost 5G IoT and Robotic Applications,” *IEEE Access*, vol. 9, pp. 11750-11760, 2021.

[13] N. Duangrit, B. Hong, A. D. Burnett, P. Akkaraekthalin, I. D. Robertson and N. Somjit, “Terahertz Dielectric Property Characterization of Photopolymers for Additive Manufacturing,” *IEEE Access*, vol. 7, pp. 12339-12347, 2019.

[14] W. Thaiwirot, P. Sangpet and P. Akkarakethalin, “A flower-shaped stub slot antenna with dual band-notched characteristics for UWB applications,” *2017 International Symposium on Antennas and Propagation (ISAP)*, 2017, pp. 1-2.